Journal of Theoretical Biology 259 (2009) 503–516

Contents lists available at ScienceDirect

Journal of Theoretical Biology

journal homepage: www.elsevier.com/locate/yjtbi

Bayesian approximations and extensions: Optimal decisions for small brains and possibly big ones too

Alexander Lange [a,b,*], Reuven Dukas [a]

[a] Department of Psychology, Neuroscience and Behaviour, McMaster University, Canada
[b] Department of Mathematics and Statistics, McMaster University, Canada

ARTICLE INFO

Article history:
Received 31 October 2008
Received in revised form
1 February 2009
Accepted 11 March 2009
Available online 5 April 2009

PACS:
51.140
71.160

Keywords:
Learning
Memory
Knowledge
Optimization
Bayes
Conditional probability
Fruit flies
Population dynamics
Computer simulation

ABSTRACT

We compared the performance of Bayesian learning strategies and approximations to such strategies, which are far less computationally demanding, in a setting requiring individuals to make binary decisions based on experience. Extending Bayesian updating schemes, we compared the different strategies while allowing for various implementations of memory and knowledge about the environment. The dynamics of the observable variables was modeled through basic probability distributions and convolution. This theoretical framework was applied to the problem of male fruit flies who have to decide which females they should court. Computer simulations indicated that, for most parameter values, approximations to the Bayesian strategy performed as well as the full Bayesian one. The linear approximation, reminiscent of the linear operator, was notably successful, and, without innate knowledge, the only successful learning strategy. Besides being less demanding in computation and thus realistic for small brains, the linear approximation was also successful at limited memory, which would translate into robustness in rapidly changing environments. Knowledge about the environment boosted the performance of the various learning strategies with maximal performance at large utilization of memory. Only for limited memory capacities, intermediate knowledge was most successful. We conclude that many animals may rely on algorithms that involve approximations rather than full Bayesian calculations because such approximations achieve high levels of performance with only a fraction of the computational requirements, in particular for extensions of Bayesian updating schemes, which can represent universal and realistic environments.

1. Introduction

Empirical research in the past few decades has established that most animals, including small-brained insects such as fruit flies (*Drosophila* spp), rely on learning to make complex decisions regarding all major life activities including feeding, predator avoidance, aggression, social interactions and sexual behavior (Dukas, 2008; Dukas and Ratcliffe, 2009; Stephens et al., 2007). Theoretical studies of animal decisions in uncertain settings have mostly relied on Bayes theorem, which is the most logically consistent method for incorporating probabilistic information (Clark and Mangel, 2000; DeGroote, 1970; Kording, 2007; McNamara et al., 2006). Whereas theoreticians widely agree about the superiority of the Bayesian method, it is not clear to what extent animals can execute Bayesian calculations, which are computationally demanding.

The two major features of the Bayesian method are, first, the notion of prior and posterior knowledge, and, second, the representation of that knowledge in terms of probability distributions that in some way map the environment. By definition, learning implies that a decision is based on the integration of prior information and current experience. This means that all animals that learn exhibit one feature of the Bayesian method. However, it is still unknown whether the animal brain represents information as problem-specific distributions such as conditional probability density functions (Dukas et al., 2006; Knill and Pouget, 2004; Rodriguez-Girones and Vasquez, 1997). Studies in humans and other animals suggest that decisions made under uncertainty are consistent with optimal choices calculated according to Bayes theorem (Fiser and Aslin, 2002; Kording and Wolpert, 2004; Valone, 2006). It is not clear, however, whether the nervous system of any animal can execute Bayesian calculations utilizing (realistic) probability distributions. That is, it is possible that animals rely on relatively simple rules when making learning-based decisions and that such decisions only resemble choices based on full Bayesian computations.

The possibility that animals rely on simple rules to reach less than optimal decisions seems especially attractive when we

* Corresponding author at: Department of Psychology, Neuroscience and Behaviour, McMaster University, 1280 Main Street West, Hamilton, Ontario, Canada L8S 4K1. Tel.: +1 905 525 9140.
E-mail address: alange.publ@gmail.com (A. Lange).

0022-5193/$ - see front matter © 2009 Elsevier Ltd. All rights reserved.
doi:10.1016/j.jtbi.2009.03.020

consider relatively simple nervous systems such as that of fruit flies, which consist of only about 200,000 neurons. However, the approximation and extensions of Bayesian rules we present in this work are by no means restricted to decisions by small brains. Students of behavior have indeed considered a variety of simple decision rules that achieve reasonable performance (Gigerenzer et al., 1999; Houston et al., 1982; Kacelnik and Krebs, 1985; McNamara et al., 2006) and there has recently been renewed interest in revealing the exact computational mechanisms employed by animals to make decisions (Gold and Shadlen, 2007; Knill and Pouget, 2004; Ydenberg et al., 2007).

There are probably three general approaches for examining decisions based on Bayesian computations. First, one can merely compare predictions based on Bayesian models to empirical data (Kording and Wolpert, 2004; Valone, 2006; van Gils et al., 2003). Whereas this approach is useful, it does not elucidate either the actual computation employed by animals or the neuronal coding that may be involved. Second, one may assume that animals can execute Bayesian calculations using probability distributions, and attempt, either theoretically or empirically, to elucidate how neuronal networks represent the necessary information and calculations (Gold and Shadlen, 2007; Holmgren and Olsson, 2000; Knill and Pouget, 2004; Kording, 2007; Yang and Shadlen, 2007). Finally, it is reasonable to assume that at least some animals cannot rely on representations of probability distributions for Bayesian calculations and instead employ some approximations that are computationally less demanding. Here we take this approach, which has received relatively little attention. Specifically, we derive explicit low-order approximations of the Bayesian strategy and find that the linear approximation performs exceptionally well compared to the full Bayesian calculations under a wide range of settings. We present our arguments tailored for mate choice problems, though we indicate that foraging, for instance, defines another class of problems where our theoretical findings can easily be translated and applied to.

The paper is divided into four sections. In the next section, we present a probabilistic optimization model, develop the concept of the Bayesian threshold and introduce fitness. We also introduce observer specific parameters, implement ultra-Bayesian updating rules, and derive Bayesian approximations. All this is illustrated for a concrete example—the mating problem of male flies, but done for unspecified distributions. In Section 3, we construct concrete probability distributions based on realistic population dynamical assumptions and apply them to the concepts introduced earlier. We utilize our example for computer simulations, comparing the Bayesian threshold strategy with its approximations. The results of these simulations are given in Section 4, demonstrating the good performance of the approximations, particularly the linear one. A discussion of our findings concludes the paper.

2. Bayesian approximations and extensions

The general problem we investigate involves an observer who has to decide how to respond to individuals of a large population that are in different states. The state of an individual is determined by a system variable but cannot be perceived by the observer without an undesired fitness cost. The observer only recognizes values of a complementing indicator variable. The relation between these two variables is directed but vague, reflecting the nature of the underlying biological processes. The observer's learning task is to predict the state of a single, arbitrarily chosen individual through the information obtained from interacting with other individuals and representing or, in a broader sense, understanding the relationship between the system and the indicator variable.

The standard example we refer to is a mating scenario: if investigated from the male's perspective, the female's state represents the objective fitness measure and the indicator variable a fitness estimate perceived by the male observer. Applications to other scenarios, where our "individuals" represent food types, food patches or nest sites instead of social partners, are possible too. The learning mechanism we describe in this section, which includes conditional decisions and a notion of fitness, is universal in biology.

2.1. Example, part 1: courtship and mating in fruit flies

The concrete example we will use to illustrate our theoretical findings is the courtship problem of fruit flies (Dukas et al., 2006). We start sketching its main biological assumptions and add more detailed description once the appropriate mathematical language is developed.

In this example, male flies are the observers who, in their limited lifetime, attempt to mate with as many female flies as possible. To this end, they have to court and be accepted as mates by the females. Courting is costly because it requires time and does not necessarily lead to mating. Therefore, the males can gain fitness if they focus their courtship efforts on the class of females most likely to accept them as mates. An indicator for possible acceptance or refusal is the pheromone concentration displayed by a female. The higher the concentration the more likely is the acceptance.

We assume that male flies can learn the relationship between the pheromone concentration and female response, keeping track of a threshold—the pheromone concentration z above which acceptance is more likely to occur than refusal. The pheromone concentration is a rough indicator for female fertility with the exception of young females, whose pheromone concentration may reach high values before sexual maturity (Manning, 1967). Besides pheromones, other indicators of acceptance might contribute to the variable z in a similar fashion. This indicator variable, which we simply assume to represent sexual attractiveness, conveys information to males about the likelihood that courting a female they encounter will be successful. The females' sexual attractiveness, however, changes over time, depending on the state females are in. For very young females (and shortly after mating) sexual attractiveness is low. It then increases (again) slowly over time (modeled mathematically in Section 3). Eventually, we are interested in studying our observers with respect to different usage of memory and of a quantity we refer to as innate knowledge, which represents information about the female population that cannot be learned through courting. (Simulation results are presented in Section 4.)

2.2. Decisions based on conditional probabilities

The system variable σ, we investigate here, is supposed to encode two distinct states $\sigma \in S = \{U, V\}$ which, interpreted as the probabilistic outcome of a revealing act, represent disjoined events, $U \cap V = \emptyset$, that span a sigma algebra $\sigma(S)$. The values attained, which are supposed to refer to positive and negative outcomes, respectively, are disclosed to the observer only after it makes a costly decision. [The courtship problem represents a straightforward application which, to ease accessibility and clarify interpretation of the more abstract terminology, we will keep indicating in square brackets throughout this section.]

The [male] observer attempts to discriminate between the two states [of female acceptance or rejection] based on the value of an

indicator variable, $x \in I = [0, y]$, representing the perceived fitness. In order to make reasonable decisions there must be a threshold value $z \in I$ such that $P(V) \geqslant P(U)$, $\forall x \geqslant z$ a.s., that is

$$P(V|x \geqslant z) \geqslant P(U|x \geqslant z). \tag{1}$$

If an observation confirms the relation, $x \geqslant z$, a costly act initiated by the observer [i.e., courting] eventually reveals the value of the system variable. For convenience, we will refer to both, the comparing value z of the indicator variable and the conditional probability $p = P(V|x \geqslant z)$ associated with the positive event V, as thresholds. We assume that the correspondence $g : I \to [0, 1]$, $z \mapsto p$ is injective (i.e., $\exists g^{-1} : p \mapsto z_p = z$). The complement, $1 - p = P(U|x \geqslant z_p)$, defines the probability associated with the event U. Therefore, relation (1) is always fulfilled if $p \geqslant \frac{1}{2}$, and the optimal probability $q = p$ for initiating the costly but overall beneficial act [of courting a promising female] is thus smaller than $\frac{1}{2}$.

To determine the specific value, $q < \frac{1}{2}$, we need to know the concrete costs and benefits of learning (investigated in Section 2.3) as well as the probability distributions of the concrete biological system. The latter would enable us to express the events $X \in \sigma(S)$ in terms of random variables x_X onto the indicator scale I,

$$x_X \sim P(x < z|X) = F_X(z), \tag{2}$$

which are distributed according to conditional probabilities, defined via cumulative distribution functions, $F_X = \mathrm{CDF}[x_X]$, over the threshold z. Despite the stochastic independence of the two events, V and U, the definitions of the corresponding biological distributions are usually not independent of each other as we will demonstrate in Section 3. The learning observer might therefore be able to consider knowledge of U as being related to knowledge of V, and vice versa.

Bayes' theorem is applied to establish the relation, $p = g(z_p)$, resolving the conditional probabilities associated with the threshold z_p,

$$p = \frac{P(V)P(x \geqslant z_p|V)}{P(x \geqslant z_p)}. \tag{3}$$

This is done by expanding the condition (i.e., the denominator) over the complete set of states (i.e., the two disjoined events),

$$P(x \geqslant z_p) = P(V)P(x \geqslant z_p|V) + P(U)P(x \geqslant z_p|U), \tag{4}$$

and expressing the threshold probability in terms of CDFs as defined in (2),

$$g(z_p) = \frac{G_V(z_p)}{G_V(z_p) + G_U(z_p)}, \tag{5}$$

where $G_V := \lambda(1 - F_V)$ and $G_U := (1 - \lambda)(1 - F_U)$, with $\lambda = P(V)$ reflecting the prevalence of state V and $1 - \lambda = P(U)$ likewise the prevalence of U.

2.3. The Bayesian fitness threshold: costs and benefits of learning

The biological context we investigate is given by the fitness of a learning observer [the male fly], determined by its overall success [i.e., the total number of mated females]. The expected fitness maximum represents an observer's optimal strategy, although, as we will discuss in Section 3.3, external factors may have an impact on the performance of an exclusively probabilistic scheme.

In our abstract formulation, observing an indicator variable, $x \geqslant z_p$, that exceeds the threshold, z_p, leads to learning about the value of the system variables, $\sigma \in S$. The process involves one non-probabilistic fitness component μ, which is a cost payable for any observation [referring to the first encounter of a female], and three probabilistic fitness components, including a cost ν conditional upon the decision to act [to court], a cost ϕ following success [acceptance], and an alternative cost ψ related to possible failure [rejection]. The expected total fitness, which is expressed as a cost here as well, adds up to

$$\begin{aligned} C_{\mathrm{tot}} &= \mu + \nu P(x \geqslant z_p) + \phi P(V \cap (x \geqslant z_p)) + \psi P(U \cap (x \geqslant z_p)) \\ &= \mu + (\nu + \phi p + \psi(1 - p))P(x \geqslant z_p) \\ &= \mu + \left(\phi + \psi + \frac{\nu + \psi}{p}\right) G_V(z_p). \end{aligned}$$

The final line was obtained utilizing Bayes' theorem, substituting expression (3) in terms of

$$P(x \geqslant z_p) = \frac{G_V(z_p)}{p}. \tag{6}$$

Costs constitute negative fitness components, modeled by the relative cost of learning subtracted by the benefit of success, $1 - \phi P(V \cap (x \geqslant z_p))/C_{\mathrm{tot}}$. The total benefit thus reads

$$B_{\mathrm{tot}} = \frac{\phi G_V(z_p)}{C_{\mathrm{tot}}(x \geqslant z_p)} \tag{7}$$

$$= \frac{1}{\frac{\phi + \psi}{\mu\phi} + \frac{1}{\phi}\left(\frac{\omega}{p} + \frac{1}{G_V(z_p)}\right)}, \tag{8}$$

where $\omega = (\nu + \psi)/\mu$. To maximize this function over the threshold candidates (either p or z_p), the following cost-related expression

$$C_{\mathrm{rel}} = \frac{\omega}{p} + \frac{1}{(G_V \circ g^{-1})(p)} \equiv \frac{\omega}{g(z_p)} + \frac{1}{G_V(z_p)} \to \min \tag{9}$$

(denoted in either formulation, and illustrated in Fig. 4A), needs to be minimized. Therefore, the condition $C'_{\mathrm{rel}}(z_q) = 0$, i.e.,

$$G_V(z_q)G'_U(z_q) - (1/\omega + G_U(z_q))G'_V(z_q) = 0 \tag{10}$$

defines the optimal threshold, $q = g(z_q)$ or z_q, if $C''_{\mathrm{rel}}(z_q) > 0$, i.e., if

$$G_V(z_q)G''_U(z_q) - (1/\omega + G_U(z_q))G'_V(z_q) > 0. \tag{11}$$

(The two conditions, given in terms of G_V and G_U, are easily verified by straightforward calculation.) It is safe to assume that such an optimal threshold,

$$z_q = b(x_U, x_V), \tag{12}$$

exists for concrete distributions of x_V and x_U (as we have demonstrated for our standard example in Appendix A.1). We can conclude that this fitness threshold only depends on costs expressed by the ratio ω, which in addition to the cost required for disclosing [courting] measures the cost of a possible negative outcome with respect to the fixed cost. In particular, the threshold is independent of the payoff from possible success.

The fitness modeling is slightly more general than needed for our example (Section 2.1), where costs are associated with times and a negative outcome does not cause an extra cost. The search time required to encounter a new possible female specifies the fixed cost μ, and the only conditional cost relevant for calculating the cost ratio ω is the courting duration, ν, i.e., $\omega = \nu/\mu$. The optimization task corresponds to maximizing the relative mating duration, which characterizes a positive fitness component, or equivalently, to minimizing the time between mating acts, which characterizes a relative cost.

Note that male flies cannot learn to optimize the threshold p as they do not know some intrinsic parameters of the optimization problem they are facing, e.g., ω. However these parameters might be fitted to the given environment through evolution. Furthermore, note that our model does not incorporate any phenotypic variation in male quality (e.g., body size, age). Therefore, calculating the average mating success is only an estimate for the real-world scenario where typically, only a small proportion of

males succeed in mating (consequently, far more often than at the average frequency).

2.4. Realistic observers and ultra-Bayesian updating

In contrast to the threshold optimization, the updating of parameters will only partially be performed according to Bayesian rules. We investigate modifications that implement imperfect memory and innate knowledge, trying to characterize more realistic observers. These "ultra-Bayesian" modifications, not to be confused with our approximation strategies, are extensions that, in our considerations here, span a two-dimensional parameter space, where, from a naive perspective, only one point, which is the case of complete memory without knowledge, represents the Bayesian approach. It is important to note that the two external scales define quantities and qualities that constrain the probabilities relevant for the fitness estimate (cf. Section 3.3). Incorporated in the probabilistic framework and less naively, the case of complete memory and total knowledge is then characterized as Bayesian, re-identifying the naive as a knowledge-free Bayesian case. The learning algorithm as outlined here is illustrated in Fig. 1.

For simplicity, we assume that information captured by the random variables, x_V and x_U, can be encoded by two numbers, $v, u \in I$, which then determine the optimal threshold $z_q = b(u, v)$. By utilizing expectation values,

$$v = \mathbb{E}(x_V) \quad \text{and} \quad u = \mathbb{E}(x_U), \tag{13}$$

the outcome [success] of an observation (with conditionally following costly act [of courting]), the nth say, is predicted by the mean value from the $n-1$ prior observations O_i, provided all have been weighted equally, $\vartheta = P(O_i) \equiv 1/n$. This statement is based on the following version of Bayes' formula (with conditional expectations),

$$\mathbb{E}(x_V) = \sum_{i \leqslant n} \mathbb{E}(x_V|O_i)P(O_i), \tag{14}$$

i.e., $v \approx \overline{v}_n \equiv (1/n)\sum_{i \leqslant n} x_V^i$, and similarly for U, where a single observation approximates its expectation, $\mathbb{E}(x_X|O_i) \approx x_V^i$. Besides linearity, an equal-weight structure identifies the optimal probabilistic approach. This structure of perfect memory is labeled

Fig. 1. The flow diagram of the learning algorithm, indicating the locations of Bayesian approximations (red) and extensions (blue). Positive feedback defines success and increases an observer's real fitness. In our model, negative feedback does not directly decrease fitness—all the costs are virtual. (For interpretation of the references to color in this figure legend, the reader is referred to the web version of this article.)

with the attribute Bayesian, but it is commonly known (Kacelnik and Krebs, 1985) that an updating rule based on real memory and indices representing time (with $i-1$ being earlier than i), is not necessarily Bayesian (i.e., $P(O_{i-1}) \neq P(O_i)$).

Intending to keep the linear structure, the update is performed as a convex combination. Information from $i-1$ observations is updated after the ith observation returns a value $x_i \in I$ for the indicator variable and a (possibly undetermined) value $\sigma_i \in \{U, V, U \cup V\}$ for the system variable (i.e., $\sigma_i = U \cup V$ if no positive decision has been made),

$$\begin{pmatrix} u_i \\ v_i \end{pmatrix} = (\mathbb{I}_2 m^i \Theta^i_{\sigma_i}) \begin{pmatrix} u_{i-1} \\ v_{i-1} \end{pmatrix} + (1 - m^i \Theta^i_{\sigma_i}) x_i, \tag{15}$$

where $\mathbb{I}_2 = \mathrm{diag}(1,1)$. The observation history is incorporated through a vector, $\Theta^i_{\sigma_i} = \Delta_{\sigma_i} \vartheta^i$ made of a matrix of Kronecker deltas

$$\Delta_{\sigma_i} = \begin{pmatrix} \delta_{U\sigma_i} & \delta_{(U\cup V)\sigma_i} \\ \delta_{(U\cup V)\sigma_i} & \delta_{V\sigma_i} \end{pmatrix} \quad \text{and} \quad \vartheta^i = \begin{pmatrix} \vartheta^i_U \\ \vartheta^i_V \end{pmatrix} \text{ with } \vartheta^i_\rho = 1/n^i_\rho \tag{16}$$

respecting the frequencies n^i_ρ of the states $\rho \in \{U, V\}$ counted during the first i observations, weighting the amount of memory utilized prior to the ith observation with the value $m^i \geqslant 0$. The ith observation is therefore memorized with a weight reciprocal to m^i. Values, $m^i > 1$ with $m^i \leqslant \min\{n^i_U, n^i_V\}$, can be used to treat negligible events. Our memory variable models the long-term usage of information and may alternatively be characterized as forgetfulness. The case $m^i = 1$, $\forall i \leqslant n$, where the maximal amount of memory is utilized and nothing is forgotten, identifies the Bayesian updating rule.

An additional parameter update is performed in order to implement innate knowledge, which is supposed to reflect information about the environment [i.e., the female population], inherited or learned earlier in an observer's life (which elsewhere we study for female mate choice, Lange and Dukas, in preparation), but beyond the ability to be learned when fulfilling the current biological task [courting]. The environmental information is assumed to be established through a dependency between the distributions of x_U and x_V, given here in terms of a correlation between the expectation values, i.e.,

$$\exists l > 0 \quad \text{such that } v = lu, \tag{17}$$

which restricts possible combinations of u and v based on the underlying population dynamics (as we will obtain in Section 3). Similar to the implementation of memory, we also extend the Bayesian updating scheme in a linear way,

$$\begin{pmatrix} u_i \\ v_i \end{pmatrix} \mapsto L K_i L^{-1} \begin{pmatrix} u_i \\ v_i \end{pmatrix}, \tag{18}$$

intertwining the estimates for the two variables, u and v, where the diagonal matrix $L = \mathrm{diag}(1, l)$ encodes the environmental constraint. The matrix

$$K_i = \begin{pmatrix} 1-\kappa^i & \kappa^i \\ \kappa^i & 1-\kappa^i \end{pmatrix} \tag{19}$$

models a convex combination (Appendix A.2) where the parameter $\kappa^i = \lambda k^i \in [0,1]$ measures the amount of knowledge $k^i > 0$ incorporated through the ith observation when respecting the observed prevalence $\lambda \approx \lambda^i$ of states (i.e., $P(V) \equiv \lambda$) in a Bayesian fashion, e.g., estimated using the thetas in (16),

$$\lambda^i = \frac{\vartheta^i_U}{\vartheta^i_U + \vartheta^i_V}. \tag{20}$$

Similar to incorporating memory, the case of $k^i = 1$, $\forall i \leqslant n$, forms the Bayesian update. No knowledge is included if $k^i = 0$, which implies no extra updating.

2.5. Approximations of the Bayesian fitness threshold

After the variables u and v, the threshold (12) which optimizes the fitness estimate according to Bayesian principles, as characterized in Sections 2.2 and 2.3, needs to be updated as well. In addition to the formal update, which is simply given by Bayesian threshold $z_i = b(u_i, v_i)$ for the updated variables, we consider approximations of this surface estimated through local expansions. Besides being available through short and universal calculations, this would enable our observers to represent the information related with the distributions of the indicator variables, x_U and x_V, by just a few numbers. The threshold update of an nth-order approximation reads

$$z_i = \sum_{0 \leqslant h+j \leqslant n} b^i_{hj} (u_i - u_{i-1})^h (v_i - v_{i-1})^j, \tag{21}$$

with coefficients $b^i_{hj} = (1/h!j!)\partial_{u^h v^j} b(u_{i-1}, v_{i-1})$, which, except for $b^i_{00} = b(u_{i-1}, v_{i-1}) = z_{i-1}$, are formed by partial derivatives at (u_{i-1}, v_{i-1}), encoding the Bayesian threshold surface b by $(n^2 + 3n + 2)/2$ numbers (e.g., 10 for order 3). Symmetries, such as those resulting from (17), may reduce the relevant numbers of coefficients even further. In situations where the correlation between u_i and v_i is known and respected completely (i.e., $k^i = 1$), there are only $n+1$ relevant coefficients.

These approximations suggest how animals could make optimal decisions while minimizing the demand on cognitive resources, especially if neural capacity is limited (Dukas, 1998, 2002). The connection to older work of the 1980s and early 1990s (Houston et al., 1982; Kacelnik and Krebs, 1985; Mangel, 1990) is obvious when looking at a special case. For vanishing knowledge, $k^i = 0$, the updating rule (15) and the observed value x_i of the indicator variable can be implemented directly in (21),

$$z_i = z_{i-1} + \sum_{1 \leqslant h+j \leqslant n} \overline{b}^i_{hj} (x_i - u_{i-1})^h (x_i - v_{i-1})^j, \tag{22}$$

where $\overline{b}^i_{hj} = b^i_{hj} (1 - \Theta^i_{\sigma_i 1})^h (1 - \Theta^i_{\sigma_i 2})^j$. Then the 1st-order approximation leads to an updating rule for the threshold that is reminiscent of the so-called linear operator, i.e.,

$$z_i = z_{i-1} + \overline{b}^i_{10}(x_i - u_{i-1}) + \overline{b}^i_{01}(x_i - v_{i-1})$$
$$\text{where } \begin{cases} \overline{b}^i_{01} = 0, \\ \overline{b}^i_{10} = 0, \\ \emptyset \end{cases} \quad \text{if } \sigma_i = \begin{cases} U, \\ V, \\ U \cup V. \end{cases} \tag{23}$$

The 0th-order approximation represents a fixed threshold, $z_i = z_0$, and therefore does not include learning.

In the next section, distributions for x_U and x_V will be generated in the context of a biological example, where we can recognize the nature of the dependencies described by L and k^i. We will investigate the performance of the Bayesian threshold model compared to its low-order approximations, up to order 3. The performance will be studied over different but constant utilization of memory and fixed amounts of knowledge, $(m^i, k^i) = (m, k)$, $\forall i$, characterizing a particular observer.

3. A population-dynamic model

The decisions investigated in the previous section, intended to increase the fitness of an observer, are based on the distribution of

an indicator variable associated with individuals in a large population, with values strongly depending on the state an individual occupies at the moment of observation. Different from a common approach in the field of applied Bayesian analysis, where standard probabilistic distributions (such as Poisson or normal distributions with known priors, etc.) are utilized, we will estimate the required distributions of x_V and x_U based on realistic assumptions about the average individual in the population.

3.1. Probability distributions obtained via convolution

The value of the system variable, which represents the current biological state of an observed individual, switches between V and U. The assumed relation between the corresponding expectations values, $u<v$, identifies the sequence (U,V) as the natural order. This convention is based on our example of mating flies (Section 2.1), where the indicator variable encodes the female's increasing attractiveness over time and the natural sequence for female behavior of first rejecting and then accepting courting males. We investigate a scenario, where the growth of the indicator variable over time periods is assumed to be constant and fixed for each state. This also applies to an auxiliary state we introduce, which defines a third value of the system variable, $W \subseteq U$, along with a corresponding random variable x_W on I. As indicated, the event W is supposed to imply U, and the sequence $(W, U\backslash W, V)$ is associated with increasing expectation values of the corresponding random variables. We propose a cyclic recurrence of the states in the latter sequence where W characterizes the recurring initial state.

Starting with distributions of the random variables, t_W, $t_{U\backslash W}$, t_V, which are supposed to model the durations of an average individual in the states, W, $U\backslash W$, V, respectively, we aim at constructing the PDFs of x_V and x_U. For the transitions between the three considered states, the summands, $t_U = t_W + t_{U\backslash W}$ and $t_{U\cup V} = t_U + t_V$, form the random variables associated with the time periods from entering the state W until leaving the state U and entering V, and leaving V and re-entering W, respectively. Noting that the addition of random variables translates as convolution of the corresponding PDFs, we obtain

$$\mathrm{PDF}[t_U] = \mathrm{PDF}[t_W] * \mathrm{PDF}[t_{U\backslash W}] \quad \text{and} \tag{24}$$
$$\mathrm{PDF}[t_{U\cup V}] = \mathrm{PDF}[t_U] * \mathrm{PDF}[t_V], \ \text{resp.} \tag{25}$$

By exploiting a linear time-dependency of the indicator variable, we can calculate the PDFs for the random variables of the states $X \in \{U,V\}$ evaluating the probabilities of the composed events of "being in X AND leaving X again" at almost any time, i.e., almost surely for any value of the indicator variable.[1] The probabilities of the AND-events are given by the products of the probability of entering X and the conditional probability of leaving X again, i.e.,

$$\mathrm{PDF}[x_U] \propto \mathrm{CDF}[t_W] \times (1 - \mathrm{CDF}[t_U]), \tag{26}$$
$$\mathrm{PDF}[x_V] \propto \mathrm{CDF}[t_U] \times (1 - \mathrm{CDF}[t_{U\cup V}]), \tag{27}$$

where the factors are expressed in terms of CDFs. Renormalization of the PDFs can be achieved via the prevalence ratio associated with the two basic states,

$$\frac{\mathrm{CDF}[x_U]}{\mathrm{CDF}[x_V]} = \frac{P(U)}{P(V)} = \frac{1}{\lambda} - 1. \tag{28}$$

The only parameter involved is the probability λ of being in V.

3.2. A simple model and its analytically treatable limiting case

Proposing the simplest scenario (Fig. 2A), we assume that the durations in the states U and V, represented by distributions of the random variables $t_{U\backslash W}$ and t_V, are given through constant densities over intervals defined by two parameters, i.e.,

$$\mathrm{PDF}[t_{U\backslash W}] \propto 1_{[\beta,\gamma]} \quad \text{and} \quad \mathrm{PDF}[t_V] \propto 1_{[0,1-\beta-\gamma]}, \tag{29}$$

where $\beta, \gamma \in I$ and $\beta<\gamma$. Without introducing new parameters, we let the initial state W be given by a slightly more complicated density—a linearly decreasing function that vanishes at β,

$$\mathrm{PDF}[t_W](z) \propto (\beta - z)1_{[0,\beta]}(z). \tag{30}$$

This choice ensures smooth PDFs for the state U (cf. the red graph in Fig. 2E), and the disjoined supports of t_W and $t_{W\backslash U}$ exclude immediate transitions from W to V. The growth rates of the indicator variable, being constant within but not necessarily equal between different states (indicated by different slopes of the vectors in Fig. 2C), are fixed implicitly by the renormalization parameter λ.

We have written a computer algebra (Wolfram Research, Inc, 2007) routine (included in `PopulationModel.nb`, Supplementary on-line material) that handles piecewise defined functions to calculate analytical expressions for the PDFs of x_V and x_U. The results are quite involved (cf. Fig. 9 in Appendix A.3)— they contain 24 and 11 rational functions in β and γ (with polynomials of up to order 6), respectively, representing coefficients in front of different Heaviside step-functions θ (which serve as basis elements). Even starting with simple initial distributions, we must acknowledge that a realistic distribution-based approach is very challenging; see the expectation value of x_V (Fig. 9) required to determine the Bayesian threshold (cf. Section 2). It is impossible to calculate analytic expressions for the two defining parameters, β and γ, depending on u and v; the determining polynomials are far beyond order four (see v and u in Fig. 9).

In order to continue with an analytical approach we must further simplify the distributions. To get simpler expressions and fewer determining parameters, we consider the limit where the duration in the state V approaches zero. (For our concrete example in Section 3.4, short stays in V are justified by a relatively low prevalence $\lambda \ll \frac{1}{2}$, which results in a high turn-over rates.) In the corresponding limit, $\beta \to 0$ and $\gamma \to 1$, (26) and (27) yield the following distributions:

$$\mathrm{PDF}[x_U](z) = 2(1-\lambda)(1-z), \tag{31}$$
$$\mathrm{PDF}[x_V](z) = 6\lambda(1-z)z, \tag{32}$$

with expectation values (cf. Fig. 2F),

$$u = \tfrac{1}{3} \quad \text{and} \quad v = \tfrac{1}{2}. \tag{33}$$

Note that these formulas are only correct for $z>0$; our limit transforms t_W into a Dirac-delta distribution and technically only the PDFs of $x_{W\backslash U}$ and x_V degenerate into a line and a parabola, respectively. Therefore, we (formally) exclude our auxiliary state $W \to \emptyset$ again (e.g., by letting $I \to (0,1]$ and compactifying) and redefine $U\backslash W \to U$ in this limiting case (Fig. 2B, D, F). Most importantly, we can now explicitly calculate (Appendix A.1) the

[1] The event of being in X includes entering X and being already in X. However, these latter two events are disjoined and therefore the probability of being in X is obtained by the sum of the probabilities of the two unified events. In the case we consider here, where the t_X are given by continuous PDFs, the probability of entering X at any chosen time vanishes, and thus we are left with the probability of being already in X. Similar arguments apply to the events associated with leaving X.

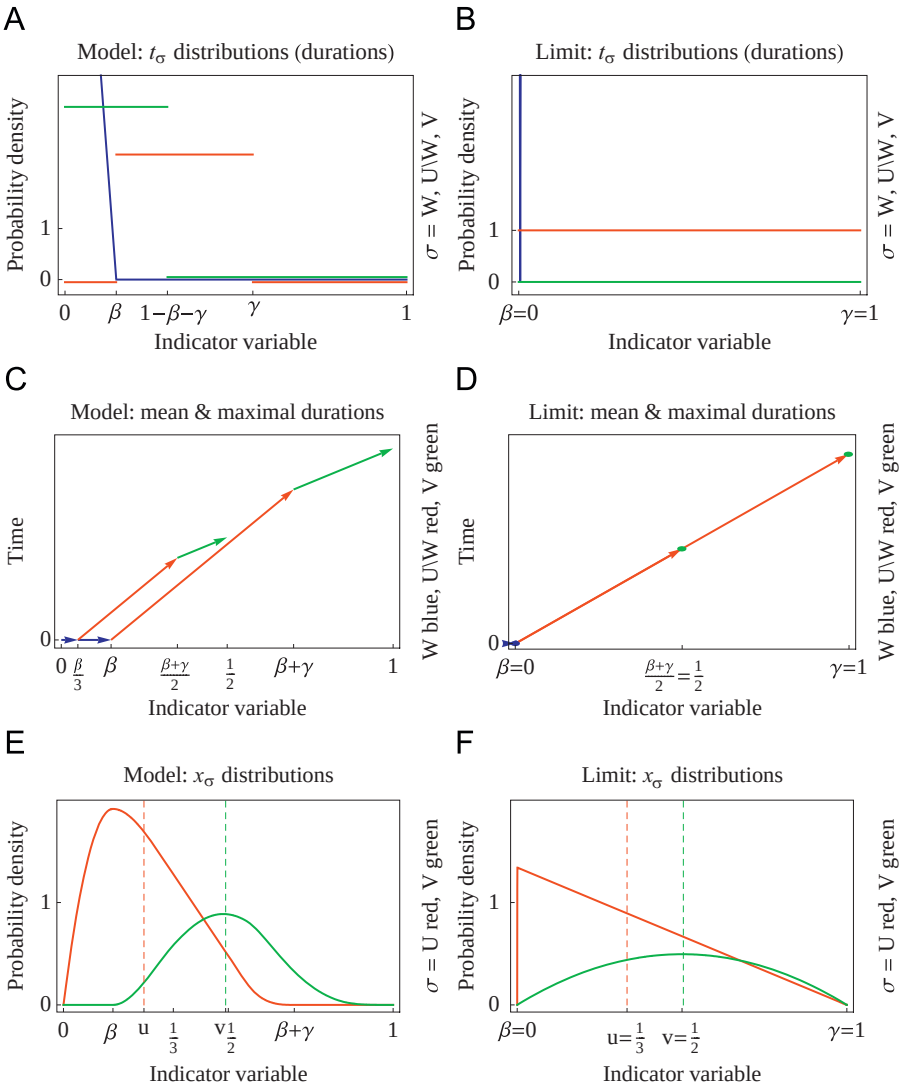

Fig. 2. The population-dynamic model (left) and its limiting case (right). (A, B) initial distributions t_σ; duration of an average individual in the states W (blue), $U\backslash W$ (red), V (blue). (C, D) indicator variables corresponding to the mean and maximal durations followed over in the states W, $U\backslash W$, V. (E, F) distributions x_σ of the indicator variable in the states U (red), V (green). (For interpretation of the references to color in this figure legend, the reader is referred to the web version of this article.)

Bayesian threshold,

$$
\begin{aligned}
b(u,v) = \frac{1}{3(\lambda-1)\omega}\Bigg(&2(6u-v)(\lambda-1)\omega \\
&+((\lambda-1)(81u^2+(3u-2v)(21u+4v)(\lambda-1)\omega)\omega) \\
&\Big/\Bigg(\Big(54(\lambda-1)^2\omega^2(5(\lambda-1)\omega+27)u^3 \\
&-27v(\lambda-1)^2\omega^2(11(\lambda-1)\omega+9)u^2 \\
&+36v^2(\lambda-1)^3\omega^2u+28v^3(\lambda-1)^3\omega^3 \\
&+\frac{1}{2}\sqrt{((\lambda-1)^3\omega^3(4(\lambda-1)\omega(243(6u-v)u^2} \\
&+(3u-2v)^2(30u+7v)(\lambda-1)\omega)^2 \\
&-4(81u^2+(3u-2v)(21u+4v)(\lambda-1)\omega)^3))\Big)^{(1/3)}\Bigg)
\end{aligned}
$$

$$
\begin{aligned}
&+\Big(54(\lambda-1)^2\omega^2(5(\lambda-1)\omega+27)u^3 \\
&-27v(\lambda-1)^2\omega^2(11(\lambda-1)\omega+9)u^2 \\
&+36v^2(\lambda-1)^3\omega^3u+28v^3(\lambda-1)^3\omega^3+\frac{1}{2}\sqrt{((\lambda-1)^3\omega^3} \\
&\times(4(\lambda-1)\omega(243(6u-v)u^2+(3u-2v)^2(30u+7v)(\lambda-1)\omega)^2 \\
&-4(81u^2+(3u-2v)(21u+4v)(\lambda-1)\omega)^3))\Big)^{(1/3)}\Bigg)
\end{aligned}
\tag{34}
$$

and its low-order approximations (Fig. 3). By utilizing computer algebraic tools one can easily find the analytic solution for the expansion coefficients b_{hj}; e.g., the 0th-order reads

$$
b_{00} = \frac{3\lambda\omega+\dfrac{3\sqrt[3]{2}(\lambda-1)\omega}{\sqrt[3]{3(\lambda-1)^2\omega^2+\sqrt{(\lambda-1)^3\omega^3(9(\lambda-1)\omega-4)}}}-3\omega+\dfrac{3\sqrt[3]{3(\lambda-1)^2\omega^2+\sqrt{(\lambda-1)^3\omega^3(9(\lambda-1)\omega-4)}}}{\sqrt[3]{2}}}{3(\lambda-1)\omega}. \tag{35}
$$

In our simulations (Section 4.1) we will consider domains $I = [0, y]$ with variable upper bound $y > 0$, which transforms the formulas above in a straightforward way. The expectation values read $u = y/3$ and $v = y/2$, but the correlation remains

$$l \equiv \frac{v}{u} = \frac{3}{2}. \tag{36}$$

3.3. Hybrid concepts: external parameters and non-probabilistic constraints

When looking for an optimal learning strategy in concrete biological settings (e.g., Section 2.1) we realized that an exclusively probabilistic approach may not be sufficient to obtain optimal decisions under realistic conditions, including the implementation of the computational method in the brain of an observer living in a complex but structured environment. We have thus introduced two deterministic parameters, memory and knowledge, and we assume that the amounts utilized cannot be controlled by the observers in the context of their learning task, where only statistical analysis is available. The values of these parameters are supposed to characterize different classes of observers. However, the two parameters are not independent of each other. Limited implementation of memory, for instance, can be interpreted as a rapidly changing environment and may neutralize the effect of knowledge.

The implementation of environmental constraints modifies the probabilistic setting and therefore also the predictions based on the Bayesian fitness threshold. Ultra-Bayesian updating will certainly influence the overall performance. A purely probabilistic (parameter-free) model relying on statistical estimates always predicts Bayesian threshold values as the optimal solution (cf. fitness contour in Fig. 4B given for the limiting case of Section 3.2 with variable upper bound $y > 0$). Bayesian threshold values, however, may not be optimal for any combination of the estimated system variables, u and v. When we start on the ridge of the fitness maximum, the optimal update for the variables, which keeps fitness maximal, points along that ridge ($\Delta v/\Delta u = 0.73$, illustrated by the black arrow and curve in Fig. 4B and C). But, if we include innate knowledge, expressed by relation (36) and weighted through updating by the parameter k, the optimal update must point away from that ridge ($\Delta v/\Delta u = \frac{3}{2}$, illustrated by the red arrow and curve in Fig. 4B and C).

We could not compare the success of the different strategies and parameter combinations by analytical means. Instead, we ran computer simulations to study the performance. We expected the Bayesian threshold strategy and its approximations to be most successful in parameter regions that incorporate the highest amounts of memory and knowledge. Furthermore, we predicted that the outcome would be shifted towards intermediate amounts of knowledge for low values of memory.

3.4. Example, part 2: the female fly population

Here we summarize our population model and explicitly identify the connection to our example modeling the courting

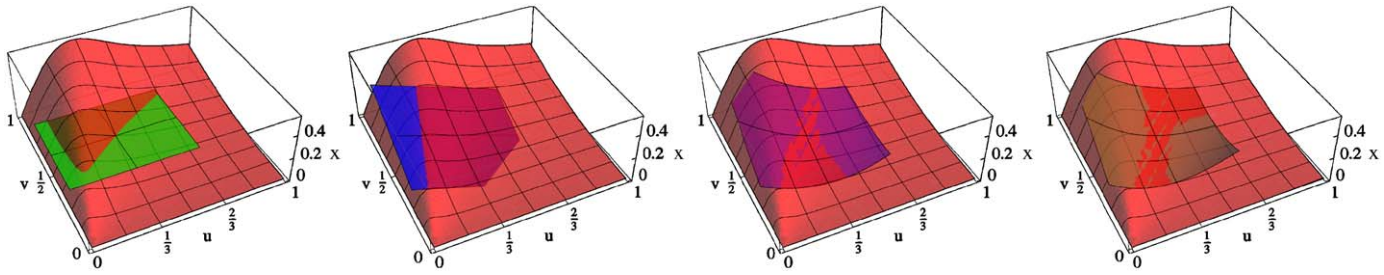

Fig. 3. The four plots illustrate the optimal Bayesian threshold (red) and its constant (green), linear (blue), quadratic (purple), and cubic (brown) approximations at $(u, v) = (\frac{1}{3}, \frac{1}{2})$, respectively, with parameters $\omega = 1$ and $\lambda = \frac{1}{100}$. (For interpretation of the references to color in this figure legend, the reader is referred to the web version of this article.)

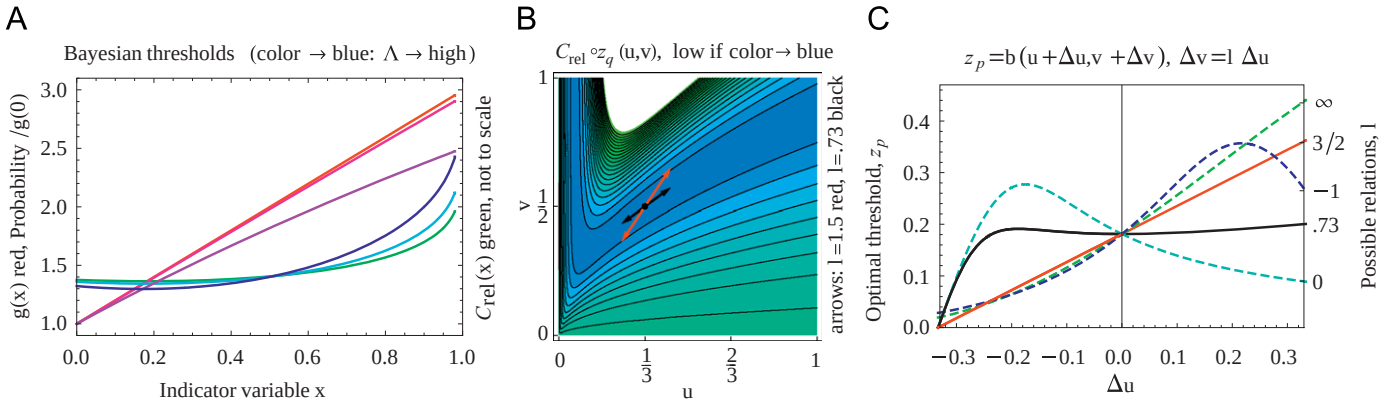

Fig. 4. (A) The reddish blue curves show the Bayesian probability threshold (normalized with respect to the frequency λ of the state V) and the greenish blue curves the relative cost C_{rel} of learning (in arbitrary units on a logarithmic scale) over I, cf. (9). The two families of curves ($-\log_{10}\lambda = 3, 2, 1$; scaled towards blue) intersect all around the optimal threshold (≈ 0.18). The relative cost is nearly constant for extended regions of the indicator variable at low values. (B) Fitness, in terms of C_{rel}, is plotted over the space of indicator variables (u, v); the bluest contour (among the black level curves) represents the optimal threshold. Corrections induced by local variations of variables, predicted according to either purely probabilistic or ultra-Bayesian updating, are indicated by black and red vectors, respectively. (C) Predicted corrections, supposed to establish optimal threshold values over deviations Δu of the observed variable u are drawn for various coefficients l (represented by different colors) in (17). Both the black and the red curve correspond to the vector of the same color in (B). The black curve is almost constant and the red curve is the only linear one. (For interpretation of the references to color in this figure legend, the reader is referred to the web version of this article.)

problem (Section 2.1)—focusing on the female individuals, the states and distributions.

A female's state was assumed to determine the indicator variable, and both these quantities were modeled to change over time. The initial state W refers to sexually unavailable females, including immature and recently mated females. Our model assigns a linearly decreasing probability density with respect to sexual attractiveness to the subpopulation in this state, cf. (30). The initial state is assumed to be an idealization. There is no finite duration of stay associated with it (i.e., horizontal arrows in Fig. 2); the female flies are supposed to go over into a state U immediately. This latter state represents either the period prior to sexual maturity or an infertile phase. From entering to leaving the state U, we assumed that the attractiveness grows linearly with time. The duration that flies are supposed to be in this state is finite; as the easiest of all possible scenarios, we assumed a constant distribution of x_U.

After a certain time each female becomes receptive and enters the state V, which is associated with an increase in female attractiveness. For simplicity, the rate of increase is again assumed to be constant. Justified by a relatively low prevalence of female flies $\lambda \ll \frac{1}{2}$ in this state of acceptance, mating occurs fast and results in high turn-over rates. Again, we model the females' duration in V by a constant density of x_V. After leaving state V, mated female flies re-enter the initial state W at a low level of sexual attractiveness, and they go through the states once again, etc.

We assume that the admissible values of the indicator variable are taken in a bounded domain, I. The ratio of probabilities describing a male's courting success or failure can be interpreted as a ratio of subpopulation sizes associated with the states, U and V; this is the right-hand-side equality of (28). In order to exclude immediate transition from W to V, the supports of the PDFs are chosen to be disjoined. Different rates are represented by different slopes of the vectors in Fig. 2, each encoding constant growth.

The biased ratio $\lambda \ll \frac{1}{2}$ is another reason why we have included innate knowledge. Through observation it is impossible to obtain an estimate for l—it is even difficult to predict a reliable estimate for λ; during their lifetime, males only mate with three females on average, as the computer simulations of the next section confirm.

4. Performance of the approximation strategies

4.1. Simulations

Following the methods developed in Sections 2 and 3, we ran computer simulations of the male fruit flies' courtship decisions presented in Sections 2.1 and 3.4 to investigate the performance of the Bayesian threshold method in comparison to its approximations. We calculated the average mating success of males over the usage of memory and knowledge for each of the four approximation strategies illustrated in Fig. 3 with individual females generated according to the distributions of the limiting case (Fig. 2B, D, F) described in Section 3.2.

Our computational resources allowed us to simulate 10,000 flies for each of the five strategies, which took about one week. It is interesting to note that the computationally demanding Bayesian strategy occupied more than half of that time. Each fly was followed up over a virtual lifetime of $t_{\text{total}} = 600$ min in total, which was divided into the following periods defining the cost parameters: $\mu = 1$ min for searching for a female, $\nu = 1$ min for courtship, $\phi = 20$ min for mating, and $\psi = 0$ if being refused. No cost was assigned to encountering an unattractive female and avoiding to court. We performed the simulations for various initial thresholds in I, and we assumed that the predicted threshold can only take positive values, which is not excluded by (21).

4.2. Results

For most of our memory-knowledge space the Bayesian threshold strategy and its linear and quadratic approximations have the highest success rates and perform equally well (Fig. 5); only for large utilization of memory and knowledge ($m, k \geqslant 0.75$), the cubic approximation leads to similar outcomes. However, for small utilization of knowledge ($k \leqslant 0.25$) and almost all ranges of memory, the linear approximation is the unique winner and performs even better than the Bayesian threshold calculations. The fixed threshold strategy represented by the constant approximation offers the best performance only for small utilization of memory ($m \leqslant 0.25$) and no knowledge ($k = 0$). Finally, for maximal utilization of memory, which corresponds to the knowledge-free Bayesian case ($m = 1, k = 0$), learning cannot improve the fixed threshold strategy; and the Bayesian strategy and the linear approximation perform equally.

All the considered learning strategies, including the Bayesian threshold and its approximations, perform well as long as the non-probabilistic environmental constraints (Section 3.3) are respected through ultra-Bayesian updating (Section 2.5), in particular for high utilization of memory ($m \geqslant 0.5$) but wide ranges of knowledge ($k \geqslant 0.25$). A stable environment, which corresponds to large utilization of memory ($m \geqslant 0.5$), favors high implementation of knowledge ($k \geqslant 0.5$), but a changing environment, corresponding to low memory ($m \leqslant 0.25$), is exploited best at an intermediate level of knowledge ($0.25 \leqslant k \leqslant 0.75$). This confirms our predictions at the end of Section 3.3.

Lower order approximations ($\leqslant 2$) are as successful as the Bayesian threshold but perform better than higher order approximations ($= 3$). Learning with good memory can compensate for possible disadvantages caused by either the strategy or the amount of knowledge implemented. Likewise, good knowledge can compensate for disadvantages caused by either the strategy or bad memory.

On an absolute scale, the effects of learning seem to be small. The maximal gain obtained by either learning method at maximal memory, high knowledge and realistic fitness parameters is between 3% and 4%. This number is large in the context of natural selection and is also larger than the magnitude of simulation errors (Fig. 6), which are smaller than 1%.

In addition to averaging over individual flies, we also averaged over initially assigned thresholds, but, except for the fixed threshold strategy, we found that the results did not depend on the initial conditions. We also ran simulations with other distributions of U and V satisfying relation (1), and obtained very similar results. It is thus plausible that our results are valid in other contexts as well.

4.3. Remarks

Our main result about the excellent performance of low-order approximations to the Bayesian threshold is not too surprising from a technical perspective. The Bayesian threshold surface is almost flat over an extended area around the point about which we perform the approximating expansions (Fig. 3). This is the case in our concrete example but might not be true in any situation, which implicitly refers to possible restrictions to the applicability of our approximation approach, namely, when the Bayesian surface incorporates high local variation.

A more differentiated view on our results raises three key questions. First, why does the linear approximation perform

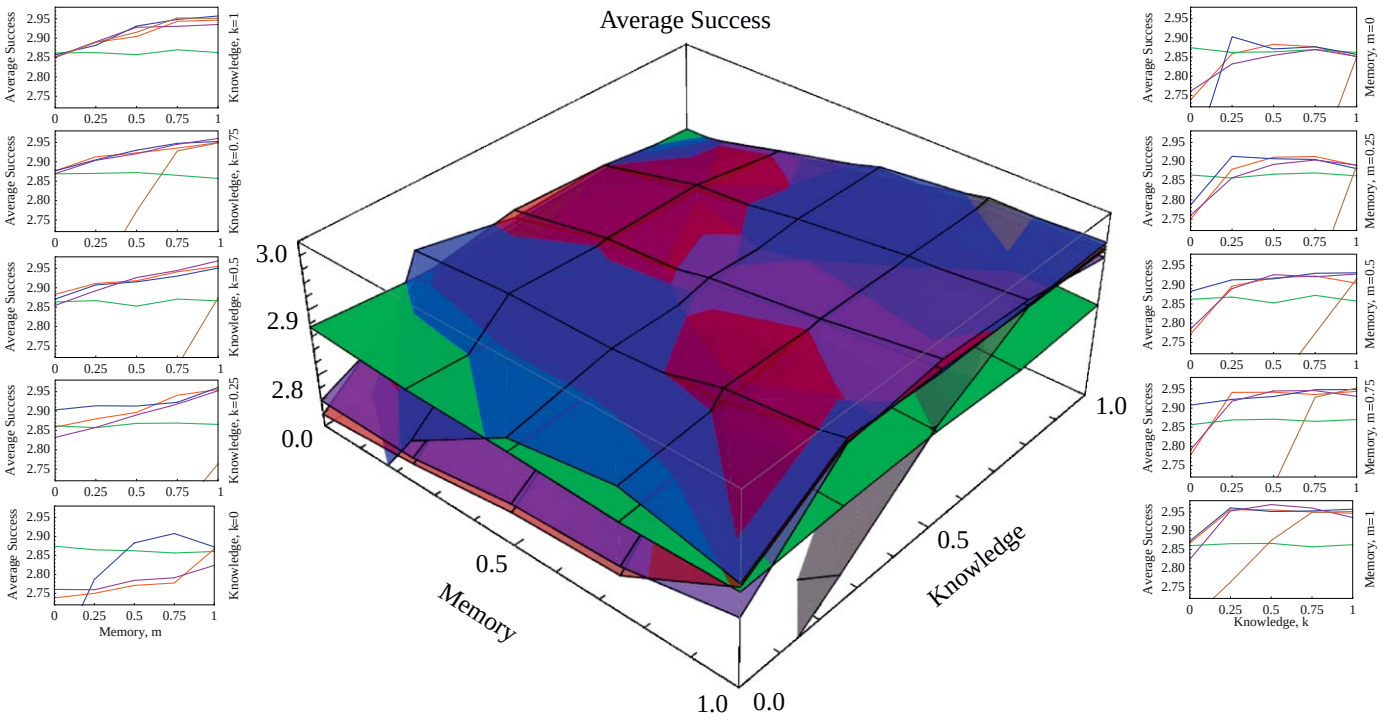

Fig. 5. Average success of the Bayesian threshold method (red) and its constant (green), linear (blue), quadratic (purple), and cubic (brown) approximations over the amounts of memory and knowledge utilized. The constant approximation shows small deviations due to stochasticity. The unsmoothed and almost constant surface illustrates the magnitude of the involved errors, which are small (cf. Fig. 6). The numerical difference between the maximal success rates of the four strategies that involve learning compared to the one that does not (green) is larger than 3%. (For interpretation of the references to color in this figure legend, the reader is referred to the web version of this article.)

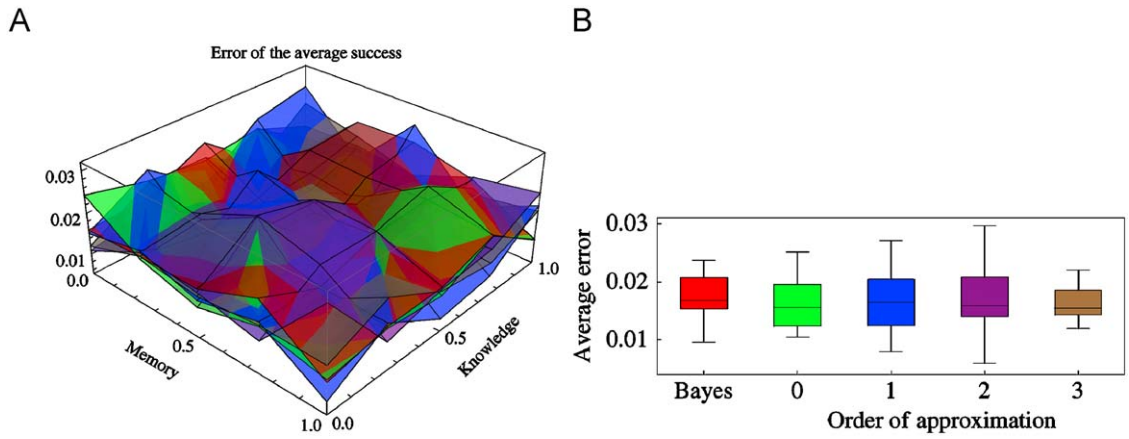

Fig. 6. (A) The stochastic error of the average success (plotted over the observer's parameter space) resulting from our computer simulations. (B) The corresponding error distribution (box-whisker) integrated over the parameter space. The maximal relative error is smaller than 1%. (Note that the figures depict the average error, not the percentage.)

better than the fully Bayesian strategy and the higher-level approximations at low innate knowledge (Fig. 5)? We think that the linear approximation is superior owing to its better ability to accommodate information that has been misperceived. The flexibility of the threshold estimation, defined by the difference of the average threshold and the estimate of the last threshold, measures this ability. Indeed our analyses indicate that the linear approximation is the most flexible algorithm when it comes to implementing small amounts of knowledge and is thus the most successful one in this region (Fig. 7B). If this is a general characteristic of the linear approximation, it may be a preferred algorithm over the full Bayesian calculations in settings with little knowledge. Our second question involves the cubic approximation, which, although of a higher order, performs poorly, except for high innate knowledge, where all learning strategies perform comparably well. Recall that the approximations are obtained by local expansions (Fig. 3). Thus we have no reason to assume that higher orders perform better (Fig. 7A). That is, the order is not a measure of quality in our context. Finally, would the linear structure (or one of the simple polynomial structures we have investigated) be successful if obtained by means other than an approximation of the Bayesian threshold? Computer simulations suggest that the Bayesian approximation is only of intermediate success but extends over the whole parameter space, whereas

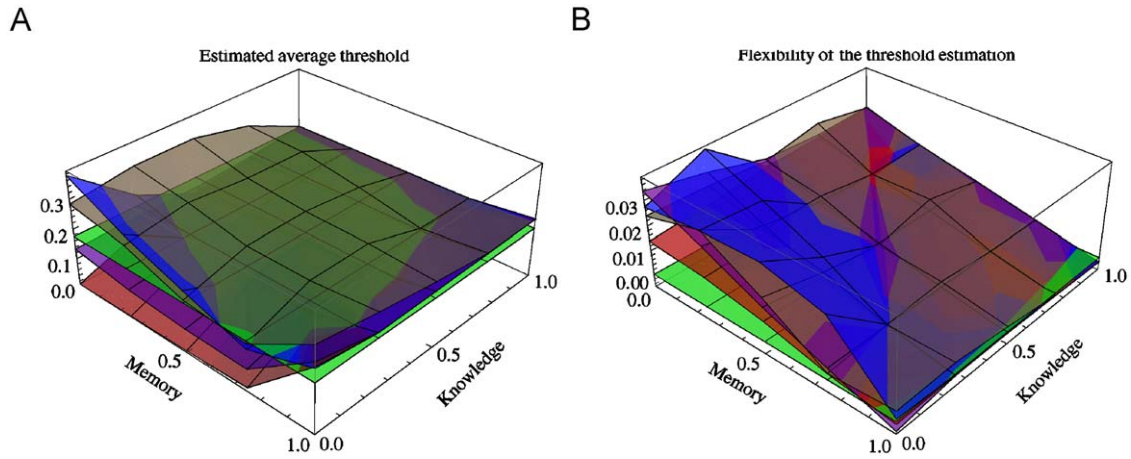

Fig. 7. (A) Estimated average thresholds for the various strategies (cf. Fig. 5, we utilize the same colors here) with respect to the amount of memory and knowledge utilized. The constant approximation (green) defines the optimal threshold. Except for the cubic approximation (brown), the optimal threshold is estimated well over large regions of memory and knowledge parameters. (B) Flexibility of the threshold estimate for the various strategies. The linear approximation (blue) is the most flexible method at low knowledge. Here, flexibility is defined as the average (over both, the runs and the various initial thresholds) of the differences between the average and the last threshold estimate. (For interpretation of the references to color in this figure legend, the reader is referred to the web version of this article.)

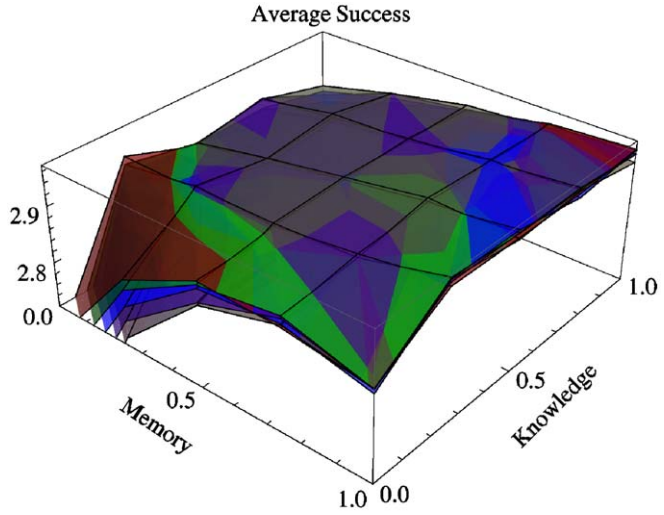

Fig. 8. Average success of the linear operator. The blue surface corresponds to the Bayesian approximation and is therefore the same blue surface as in Fig. 5. The other four surfaces correspond to small modifications of the Bayesian coefficients, from −10% (red) to +10% (brown) for both linear coefficients simultaneously. The Bayesian approximation is of intermediate success, but the modifications dominate only for certain parameter combinations; for example, the red modification is more successful for low values of memory and knowledge, whereas the brown is more successful for high values. (For interpretation of the references to color in this figure legend, the reader is referred to the web version of this article.)

modifications can be more successful but only within limited parameter regions (Fig. 8).

5. Discussion

We have investigated a learning problem involving an observer that makes costly decisions that can increase its fitness. We approached the solution to this optimization problem utilizing a threshold method based on Bayesian principles. As our main result, we found that low-order approximations to the Bayesian threshold perform as well as the full Bayesian calculations (Fig. 5). Among these approximations, we highlight the one with the simplest structure, the linear approximation, which performs particularly well when either memory or innate knowledge are limited. Approximations have two major advantages over the full Bayesian calculations. First, they have much lower memory requirements because they handle numbers rather than distributions (22). Second, they involve simpler, shorter calculations compared to the full Bayesian approach, as illustrated by the length of (34) versus (23). These properties make approximations attractive candidates for the method implemented by real nervous systems.

To examine the performance of different observers, we have extended the probabilistic description and developed an ultra-Bayesian updating algorithm. We assumed that observers are characterized by two interrelated parameters modeling the memory capacities and innate knowledge, which cannot be optimized through learning. The implementation of these hybrid concepts indicated that, for a realistic environment involving internal dynamics, performance is not optimal if observers rely only on genuinely probabilistic principles (Fig. 4). Ultra-Bayesian updating outperforms fitness maximization estimated via thresholds and produces non-trivial performance surfaces (Fig. 5). Depending on the level of memory, the adequate amount of knowledge always improves the overall success rate. For both the Bayesian threshold strategy and its approximations, we found that good memory compensates for bad knowledge and vice versa. Bad memory, however, requires only intermediate knowledge to achieve best performance (Fig. 5), whereas perfect memory in the knowledge-free case, representing the totally Bayesian updating scheme, does not allow either the full Bayesian algorithm or its approximations to perform better than the fixed threshold strategy (Fig. 5).

In addition to utilizing non-probabilistic elements for solving the optimization problem, we used non-standard probabilistic methods for modeling the distributions defining the system settings relevant for our observers. Unlike most studies in the field which, for example, utilize normal distributions, we constructed the relevant distributions based on assumptions about the internal dynamics of the environment. We started from initial distributions, which define the durations of individuals in the relevant states, and calculated their propagation in time using basic mathematical concepts such as convolution products (Section 3.1). We had to apply computer algebraic methods to obtain analytic expressions for these realistic distributions (Fig. 2E). This illustrates a universal aspect of modeling

realism—complication, which forced us to utilize approximations. In fact, we performed our simulations for a limiting case. These limiting distributions, however, preserved the important quality relating to the underlying system (Fig. 2), namely, dependencies reflecting environmental constraints, cf. (36). Performance, as discussed above, crucially depends on how decisions are made based on knowledge about the environment.

Several previous studies used modeling techniques as simple as our linear approximations. Bush and Mosteller (1951) assumed that learning causes a linear transformation in the probability of a

$$
\begin{aligned}
\mathrm{PDF}(x_V) = {} & -\frac{(x-\gamma)\left(x^2-3\beta x-2\gamma x+3\beta^2+\gamma^2+3\beta\gamma\right)\theta(x-2\beta,\gamma-x)\,(x-2\beta)^4}{36\beta^4(\beta-\gamma)^2(\beta+\gamma-1)}+\\
& \frac{1}{36\beta^4(\beta-\gamma)^2(\beta+\gamma-1)}\left(3(\beta-\gamma)x^3+3\left(-2\beta^2+4\gamma\beta+\gamma^2\right)x^2-\gamma\left(15\beta^2+9\gamma\beta+\gamma^2\right)x+\right.\\
& \left.\beta\left(-9\beta^3+6(\gamma+2)\beta^2+6\gamma(3\gamma-2)\beta+2\gamma^3\right)\right)\theta(x-2\beta)\,(x-2\beta)^3+\\
& \left((x-\gamma)\left(x^3-(4\beta+3\gamma)x^2+\left(-3\beta^2+8\gamma\beta+3\gamma^2\right)x+6\beta^3-\gamma^3-4\beta\gamma^2\right)\right.\\
& \left.\theta(x-2\beta,x-\gamma)\,(x-2\beta)^3\right)\Big/\left(36\beta^4(\beta-\gamma)^2(\beta+\gamma-1)\right)+\\
& \frac{(x+\gamma-1)^3\,(x-4\beta+\gamma-1)\,\theta(x-2\beta,x+\gamma-1)\,(x-2\beta)^3}{36\beta^4(\beta-\gamma)^2(\beta+\gamma-1)}+\\
& \frac{(\gamma-x)\left(x^2-3\beta x-2\gamma x+3\beta^2+\gamma^2+3\beta\gamma\right)}{3\beta^2(\beta-\gamma)}-\frac{1}{36\beta^4(\beta-\gamma)^2(\beta+\gamma-1)}\\
& (x-\beta)^2\left(3(\beta-\gamma)x^4+3\left(-8\beta^2+8\gamma\beta+\gamma^2\right)x^3+\left(55\beta^3-54\gamma\beta^2-21\gamma^2\beta-\gamma^3\right)x^2+\right.\\
& \left.3\beta\left(-22\beta^3+4(4\gamma+1)\beta^2+\gamma(15\gamma-4)\beta+2\gamma^3\right)x+\right.\\
& \left.\beta^2\left(68\beta^3-3(5\gamma+16)\beta^2+3(16-21\gamma)\gamma\beta-5\gamma^3\right)\right)\theta(x-\beta)-\\
& \frac{(x-3\beta-1)\,(x+\beta-1)^3\left(3x^2-3(3\beta+\gamma)x+(2\beta+\gamma)^2\right)\theta(x+\beta-1)}{36\beta^4(\beta-\gamma)(\beta+\gamma-1)}+\\
& \frac{1}{36\beta^4(\beta-\gamma)^2(\beta+\gamma-1)}\left(3(\beta-\gamma)x^6+\left(-18\beta^2+6\gamma\beta+15\gamma^2\right)x^5+\right.\\
& \left.\left(16\beta^3+45\gamma\beta^2-57\gamma^2\beta-31\gamma^3\right)x^4+2\left(19\beta^4-50\gamma\beta^3-3\gamma^2\beta^2+56\gamma^3\beta+17\gamma^4\right)x^3-\right.\\
& \left.3\left(16\beta^5+2\gamma\beta^4-44\gamma^2\beta^3+20\gamma^3\beta^2+33\gamma^4\beta+7\gamma^5\right)x^2+\right.\\
& \left.(51\beta^6+12(4\gamma-3)\beta^5+12(3-7\gamma)\gamma\beta^4-52\gamma^3\beta^3+51\gamma^4\beta^2+42\gamma^5\beta+7\gamma^6)x-\right.\\
& \left.\gamma\left(51\beta^6-36\beta^5+4(9-13\gamma)\gamma\beta^4-4\gamma^3\beta^3+12\gamma^4\beta^2+7\gamma^5\beta+\gamma^6\right)\right)\\
& \theta(x-\gamma)+\frac{1}{36\beta^4(\beta-\gamma)^2(\beta+\gamma-1)}(-x+\beta+\gamma)^3\\
& \left(x^4-4(\beta+\gamma)x^3+6(\beta+\gamma)^2x^2-\left(19\beta^3-3\gamma\beta^2+12\gamma^2\beta+4\gamma^3\right)x+\right.\\
& \left.2\beta^4+\gamma^4+12\beta^3+4\beta\gamma^3+3\beta^2\gamma(3\gamma-4)\right)\theta(x-\beta-\gamma)+\\
& \frac{(x-\gamma)\left(x^2-3\beta x-2\gamma x+3\beta^2+\gamma^2+3\beta\gamma\right)\theta(\gamma-x)}{3\beta^2(\beta-\gamma)}+\frac{1}{36\beta^4(\beta-\gamma)^2(\beta+\gamma-1)}\\
& (x+\gamma-1)^3\left(-16\beta^4+4(4\gamma-1)\beta^3+3\gamma(3\gamma+1)\beta^2+\gamma^2(\gamma+3)\beta-(\gamma-1)\gamma^3+3x^3(\beta-\gamma)-\right.\\
& \left.3x^2\left(6\beta^2-7\gamma\beta+\beta-\gamma\right)+x\left(28\beta^3+(6-33\gamma)\beta^2-3\gamma(3\gamma+2)\beta+\gamma^2(2\gamma-3)\right)\right)\\
& \theta(x+\gamma-1)+\frac{1}{36\beta^4(\beta-\gamma)^2(\beta+\gamma-1)}(x-\beta+\gamma-1)^4\\
& \left(-x^3+3(\beta+\gamma)x^2-3\left(2\beta^2+2\gamma\beta+\gamma^2\right)x+4\beta^3+\gamma^3+3\beta\gamma^2+3\beta^2\gamma\right)\theta(x-\beta+\gamma-1)-\\
& \frac{(x-3\beta-1)\left(x^2-(\beta+1)x-2(\beta-1)\beta\right)^3\theta(x-2\beta,x+\beta-1)}{36\beta^4(\beta-\gamma)^2(\beta+\gamma-1)}+\\
& \frac{(x-5\beta)\,(x-\beta)^3\,(x-\gamma)\left(x^2-3\beta x-2\gamma x+3\beta^2+\gamma^2+3\beta\gamma\right)\theta(x-\beta,\gamma-x)}{36\beta^4(\beta-\gamma)^2(\beta+\gamma-1)}+\\
& \frac{(x-3\beta-1)\,(x+\beta-1)^3\,(x-\beta-\gamma)^3\,\theta(x+\beta-1,x-\beta-\gamma)}{36\beta^4(\beta-\gamma)^2(\beta+\gamma-1)}+\\
& \frac{(x-3\beta-1)\,(x+\beta-1)^3\,(x-\gamma)\left(x^2-3\beta x-2\gamma x+3\beta^2+\gamma^2+3\beta\gamma\right)\theta(x+\beta-1,\gamma-x)}{36\beta^4(\beta-\gamma)^2(\beta+\gamma-1)}+\\
& \frac{1}{36\beta^4(\beta-\gamma)^2(\beta+\gamma-1)}\\
& (x-\gamma)^4\left(-x^3+(7\beta+3\gamma)x^2-\left(15\beta^2+14\gamma\beta+3\gamma^2\right)x+12\beta^3+\gamma^3+7\beta\gamma^2+15\beta^2\gamma\right)\\
& \theta(x-\gamma,\gamma-x)-\frac{(x-\gamma)\,(x+\gamma-1)^3\,(x-4\beta+\gamma-1)\,\theta(x-\gamma,x+\gamma-1)}{12\beta^2(\beta-\gamma)^2(\beta+\gamma-1)}+\\
& \frac{(x-\gamma)\,(x-\beta+\gamma-1)^4\,\theta(x-\gamma,x-\beta+\gamma-1)}{12\beta^2(\beta-\gamma)^2(\beta+\gamma-1)}+\\
& \frac{(x-\gamma)\,(-x+\beta+\gamma)^4\left(x^2-3\beta x-2\gamma x+3\beta^2+\gamma^2+3\beta\gamma\right)\theta(x-\beta-\gamma,\gamma-x)}{36\beta^4(\beta-\gamma)^2(\beta+\gamma-1)}-\\
& \frac{(x-\beta-\gamma)^3\,(x+\gamma-1)^3\,(x-4\beta+\gamma-1)\,\theta(x-\beta-\gamma,x+\gamma-1)}{36\beta^4(\beta-\gamma)^2(\beta+\gamma-1)}-\\
& \frac{(x-\beta+\gamma-1)^4\,(-x+\beta+\gamma)^3\,\theta(x-\beta-\gamma,x-\beta+\gamma-1)}{36\beta^4(\beta-\gamma)^2(\beta+\gamma-1)}+\frac{1}{36\beta^4(\beta-\gamma)^2(\beta+\gamma-1)}\\
& (x-\gamma)\,(x+\gamma-1)^3\left(-x^3+(7\beta+\gamma+1)x^2+\left(-15\beta^2-(8\gamma+3)\beta+(\gamma-2)\gamma\right)x+\right.\\
& \left.12\beta^3-(\gamma-1)\gamma^2+\beta\gamma(\gamma+3)+\beta^2(9\gamma+3)\right)\theta(\gamma-x,x+\gamma-1)+\\
& \frac{(x-\gamma)\,(x-\beta+\gamma-1)^4\left(x^2-3\beta x-2\gamma x+3\beta^2+\gamma^2+3\beta\gamma\right)\theta(\gamma-x,x-\beta+\gamma-1)}{36\beta^4(\beta-\gamma)^2(\beta+\gamma-1)}
\end{aligned}
$$

$$
\begin{aligned}
\mathrm{PDF}[x_U] = {} & \frac{(x-4\beta)\,\theta(x-\beta,\beta-x)\,(x-\beta)^4}{3\beta^4(\beta-\gamma)}-\frac{(x-4\beta)\,\theta(x-\beta)\,(x-\beta)^2}{3\beta^2(\beta-\gamma)}-\\
& \frac{\theta(\beta-x)\,(x-\beta)^2}{\beta^2}-\frac{(x-2\beta)^3\,\theta(x-2\beta,\beta-x)\,(x-\beta)^2}{3\beta^4(\beta-\gamma)}+\\
& \frac{(x-\gamma)\,\theta(\beta-x,x-\gamma)\,(x-\beta)^2}{\beta^2(\beta-\gamma)}+\frac{(x-\beta-\gamma)^3\,\theta(\beta-x,x-\beta-\gamma)\,(x-\beta)^2}{3\beta^4(\beta-\gamma)}+\\
& \frac{x^3-3(\beta+\gamma)x^2+3(\beta+\gamma)^2x+3\beta^3-\gamma^3-3\beta\gamma^2-6\beta^2\gamma}{3\beta^2(\beta-\gamma)}+\\
& \frac{(x-2\beta)^3\,\theta(x-2\beta)}{3\beta^2(\beta-\gamma)}+\frac{(\gamma-x)\,\theta(x-\gamma)}{\beta-\gamma}+\frac{(-x+\beta+\gamma)^3\,\theta(x-\beta-\gamma)}{3\beta^2(\beta-\gamma)}+\\
& \frac{(\gamma-x)\left(x^2-3\beta x-2\gamma x+3\beta^2+\gamma^2+3\beta\gamma\right)\theta(\gamma-x)}{3\beta^2(\beta-\gamma)}
\end{aligned}
$$

$$
\begin{aligned}
v = {} & \left(-\frac{(7\beta+\gamma)\,\theta(2\beta-\gamma)\,(\gamma-2\beta)^8}{90\,720\beta^4(\beta-\gamma)^2(\beta+\gamma-1)}+\frac{1}{90\,720\beta^4(\beta-\gamma)^2(\beta+\gamma-1)}\right.\\
& \left(-26\,973\beta^9+9(101\gamma+2848)\beta^8+792\left(38\gamma^2-44\gamma+27\right)\beta^7-\right.\\
& 168\left(15\gamma^3+132\gamma^2-189\gamma+202\right)\beta^6-252\left(105\gamma^4-184\gamma^3+102\gamma^2+8\gamma-56\right)\beta^5-\\
& 252\left(55\gamma^5-40\gamma^4-90\gamma^3+140\gamma^2-80\gamma+24\right)\beta^4-672(\gamma-1)^5(\gamma+2)\beta^3+72(\gamma-1)^7\\
& \left.\beta^2+9(\gamma-1)^7(5\gamma+3)\beta+(\gamma-1)^8(5\gamma+4)\right)+\frac{(3\beta-1)^7\left(9\beta^2+15\beta+2\right)\theta(3\beta-1)}{45\,360\beta^4(\beta-\gamma)^2(\beta+\gamma-1)}-\\
& \frac{(2\beta+\gamma-1)^7\left(2\beta^2-(25\gamma+29)\beta+5\gamma^2-\gamma-4\right)\theta(-2\beta-\gamma+1)}{90\,720\beta^4(\beta-\gamma)^2(\beta+\gamma-1)}-\\
& \frac{\left(26\beta^2-19(\gamma-1)\beta+2(\gamma-1)^2\right)(2\beta+\gamma-1)^7\,\theta(2\beta+\gamma-1)}{45\,360\beta^4(\beta-\gamma)^2(\beta+\gamma-1)}+\\
& \frac{(1-2\gamma)^6\left(-36(\gamma+3)\beta^2+9(1-2\gamma)^2\beta+(1-2\gamma)^2(\gamma+4)\right)\theta(2\gamma-1)}{45\,360\beta^4(\beta-\gamma)^2(\beta+\gamma-1)}+\\
& \frac{(\beta-2\gamma+1)^7\left(23\beta^2+(25\gamma+19)\beta+2\gamma^2+7\gamma-4\right)\theta(-\beta+2\gamma-1)}{90\,720\beta^4(\beta-\gamma)^2(\beta+\gamma-1)}+\\
& \left.\frac{(\beta+2\gamma-1)^7\left(31\beta^2+(37-11\gamma)\beta-2\gamma^2-7\gamma+4\right)\theta(\beta+2\gamma-1)}{90\,720\beta^4(\beta-\gamma)^2(\beta+\gamma-1)}\right)\Big/\\
& \left(\frac{(5\beta+1)\,\theta(3\beta-1)\,(3\beta-1)^7}{10\,080\beta^4(\beta-\gamma)^2(\beta+\gamma-1)}+\frac{1}{10\,080\beta^4(\beta-\gamma)^2(\beta+\gamma-1)}\right.\\
& \left(-6508\beta^8-160(2\gamma-79)\beta^7+112\left(33\gamma^2-26\gamma-77\right)\beta^6-336\left(3\gamma^3+6\gamma^2-6\gamma-8\right)\beta^5-\right.\\
& \left.140\left(47\gamma^4-104\gamma^3+84\gamma^2-32\gamma+8\right)\beta^4-224(\gamma-1)^5\beta^3+8(\gamma-1)^7\beta+(\gamma-1)^8\right)+\\
& \frac{(6\beta-\gamma+1)\,(2\beta+\gamma-1)^7\,\theta(-2\beta-\gamma+1)}{10\,080\beta^4(\beta-\gamma)^2(\beta+\gamma-1)}-\frac{(6\beta-\gamma+1)\,(2\beta+\gamma-1)^7\,\theta(2\beta+\gamma-1)}{10\,080\beta^4(\beta-\gamma)^2(\beta+\gamma-1)}+\\
& \frac{\left((1-2\gamma)^2-28\beta^2\right)(1-2\gamma)^6\,\theta(2\gamma-1)}{5040\beta^4(\beta-\gamma)^2(\beta+\gamma-1)}+\frac{(\beta-2\gamma+1)^7\,(7\beta+2\gamma-1)\,\theta(-\beta+2\gamma-1)}{10\,080\beta^4(\beta-\gamma)^2(\beta+\gamma-1)}+\\
& \left.\left.\frac{(7\beta-2\gamma+1)\,(2\beta+2\gamma-1)^7\,\theta(\beta+2\gamma-1)}{10\,080\beta^4(\beta-\gamma)^2(\beta+\gamma-1)}\right)\right.,
\end{aligned}
$$

$$
u = \frac{2\beta^2+2\gamma\beta+\gamma^2}{3(\beta+\gamma)}
$$

Fig. 9. PDFs (un-normalized) and expectation values of the full (β,γ)-population model (calculated in `PopulationModel.nb`, Supplementary on-line material).

subject exhibiting a certain response. The linear operator was further explored in behavioral ecology (Kacelnik and Krebs, 1985; McNamara and Houston, 1987). Mangel (1990) and McNamara and colleagues (Collins et al., 2006; McNamara et al., 2006) used linear transformations within a Bayesian framework, relying on the fact that parameters defining the distributions utilized there are concatenated via linear operations when updated (DeGroote, 1970, p. 229). To our knowledge, neither the linear operator nor the polynomial structures have been investigated as approximations to Bayesian calculations. Unlike the approaches quoted above, which all use standard probabilistic distributions, our Bayesian threshold model is built upon distributions tailored to the underlying population dynamics. Importantly, the resulting distributions, which are less standard in appearance (Fig. 2), are not independent of each other. We have also seen huge numerical complexity (Fig. 9), even when calculating the Bayesian threshold with simplified distributions (34). However, decisions based on approximations do not require the observer to determine the Bayesian threshold. This adds another important aspect: the mathematical structure of the approximations is universal (22). Non-Bayesian realizations may even perform better than their Bayesian counterparts for certain parameter regions. The linear approximation (Fig. 7B) and its non-Bayesian realizations (Fig. 8) are very successful at low memory, meaning that it can be a robust strategy in rapidly changing environments. Most remarkably, in the absence of knowledge, the linear approximation turns out to be the only successful learning strategy. All this suggests that the structural foundation underlying decisions involving learning may be as simple as the linear operator introduced half a century ago by Bush and Mosteller (1951).

The linear as well as the other low-order polynomial structures offer high levels of plasticity. Besides their realization as Bayesian approximations, explaining the good performance (Fig. 7B) as detailed for the linear approximation in Section 4.3, we also emphasize their easy implementation (Fig. 8). An animal's brain needs to encode only a few numbers: observations are weighted by a few coefficients, b^i_{hj} in (22), estimating thresholds that immediately lead to optimized decisions. We cannot further describe how these numbers, the different strategies, or the decision algorithm are encoded in an animal brain, though we believe that the simplicity and the performance, for the linear approximation in particular, would be especially attractive for animals with small brains and limited computational ability. Nevertheless, due to its efficiency, this simple structure may be used by organisms with elaborate cognitive abilities as well because they could allow improved performance owing, for example, to optimizing the use of expensive brain tissue, or the ability to execute faster decisions.

We have demonstrated that approximations of Bayesian strategies as well as extensions of Bayesian updating are powerful alternatives to completely Bayesian algorithms, which, besides being computationally demanding, are rather unrealistic for their purpose. The concrete example we investigated suggests that a linear approximation, which performs best with intermediate levels of memory and knowledge, encodes good strategies for small brains such as those of fruit flies and could be as successful even for animals with greater cognitive abilities. We should note that, because the approximations performed as well as the full Bayesian threshold strategies for most parameter values, empirical studies testing theoretical predictions derived via Bayesian calculations cannot easily inform us whether subjects employ full Bayesian or simpler approximation methods. In the knowledge-free case, however, we identified the linear approximation as the only profitable learning strategy.

Acknowledgment

We thank the anonymous reviewers for their useful comments, which helped in improving the coverage and the accessibility of our manuscript.

Appendix A

A.1. The optimal threshold of the limiting case

For the limiting case of our population model, the relative cost reads

$$C_{\mathrm{rel}}(z)=\frac{9\omega\lambda(z-3v)u^2z^2+4\omega(1-\lambda)(z-6u)v^3z+36(1+\omega)u^2v^3}{9\lambda u^2(z-2v)(z+v)^2} \tag{37}$$

$$=\frac{1+\omega(1+2\lambda z)(1-z)^2}{\lambda(1+2z)(1-z)^2}. \tag{38}$$

After simplification, (10) can be written as

$$0=-27u^2z_q+\omega(1-\lambda)(z_q-3u)(4v^2+z_q(z_q-9u+2v)) \tag{39}$$

$$=-3z_q+\omega(1-\lambda)(1-z_q)^3. \tag{40}$$

Being a cubic equation, we can calculate its roots explicitly (`BayesianThreshold.nb`, Supplementary on-line material); the relevant roots are given by (34) and (35). Utilizing inequality (11), i.e.,

$$0<27u^2(v-z_q)+\omega(1-\lambda)(4v^3+u(27u-18z_q)(v-z_q)-2z_q^3) \tag{41}$$

$$=3(1-2z_q)+4\omega(1-\lambda)(1-z_q)^3, \tag{42}$$

we can confirm that z_q is an optimal threshold, namely if

$$z_q\leqslant v \quad\text{and}\quad z_q\leqslant 3u/2,\ \text{i.e., } z_q\leqslant 1/2. \tag{43}$$

Notice the threshold's independence from cost and population size parameters.

A.2. Ultra-Bayesian updating: knowledge through convex combination

The update of u and v after the ith observation incorporates knowledge k^i through a convex combination,

$$\begin{pmatrix}u_i\\v_i\end{pmatrix}\mapsto k^i\begin{pmatrix}\Delta u_i\\\Delta v_i\end{pmatrix}+(1-k^i)\begin{pmatrix}u_i\\v_i\end{pmatrix}, \tag{44}$$

where also the updating correction is encoded through convex combinations,

$$\begin{pmatrix}\Delta u_i\\\Delta v_i\end{pmatrix}=\begin{pmatrix}1-\lambda\\\lambda\end{pmatrix}u_i+\begin{pmatrix}\lambda\\1-\lambda\end{pmatrix}v_i=\begin{pmatrix}1-\lambda&\lambda\\\lambda&1-\lambda\end{pmatrix}\begin{pmatrix}u_i\\v_i\end{pmatrix}, \tag{45}$$

respecting the frequency λ of states in a Bayesian fashion. Together, we obtain a single convex combination in terms of the parameter $\kappa^i=\lambda k^i$,

$$\begin{pmatrix}u_i\\v_i\end{pmatrix}\mapsto k^i\begin{pmatrix}1-\lambda&\lambda\\\lambda&1-\lambda\end{pmatrix}\begin{pmatrix}u_i\\v_i\end{pmatrix}+(1-k^i)\begin{pmatrix}u_i\\v_i\end{pmatrix} \tag{46}$$

$$=\begin{pmatrix}1-\lambda k^i&\lambda k^i\\\lambda k^i&1-\lambda k^i\end{pmatrix}\begin{pmatrix}u_i\\v_i\end{pmatrix}. \tag{47}$$

A.3. Formulas of the population-dynamic model

The PDFs of the population-dynamic model containing the two parameters β and γ can be expressed analytically (Fig. 9) with

expectation values different from the limiting case (33). Besides the complexity involved when dealing with more realistic distributions, one realizes conceptual problems. For a given set of expectation values, u and v (estimated through mean values), it is impossible to solve for β and γ analytically. Nevertheless, the full population model could be applied in numerical simulations.

Appendix B. Supplementary data

Supplementary data associated with this article can be found in the online version at 10.1016/j.jtbi.2009.03.020.

References

Bush, R.R., Mosteller, F., 1951. A mathematical model for simple learning. Psychological Review 58, 313–323.

Clark, C.W., Mangel, M., 2000. Dynamic State Variable Models in Ecology. Oxford University Press, New York.

Collins, E.J., McNamara, J.M., Ramsey, D.M., 2006. Learning rules for optimal selection in a varying environment: mate choice revisited. Behavioral Ecology 17, 799–809.

DeGroote, M.H., 1970. Optimal Statistical Decisions. McGraw-Hill, New York.

Dukas, R., 1998. Constrainsts on information processing and their effects on behaviour. In: Dukas, R., (Ed.), Cognitive Ecology, University of Chicago Press, Chicago, pp. 89–127.

Dukas, R., 2002. Behavioural and ecological consequences of limited attention. Philosophical Transactions of the Royal Society of London B 357, 1539–1548.

Dukas, R., 2008. Evolutionary biology of insect learning. Annual Review of Entomology 53, 145–160.

Dukas, R., Clark, C.W., Abbott, K., 2006. Courtship strategies of male insects: When is learning advantageous? Animal Behaviour 72, 1395–1404.

Dukas, R., Ratcliffe, J., 2009. Cognitive Ecology II. University of Chicago Press, Chicago.

Fiser, J., Aslin, R.N., 2002. Statistical learning of new visual feature combinations by infants. Proceedings of the National Academy of Sciences USA 99, 15822–15826.

Gigerenzer, G., Todd, P.M., Group, A.R., 1999. Simple Heuristics that Make us Smart. Oxford University Press, Oxford.

Gold, J.I., Shadlen, M.N., 2007. The neural basis of decision making. Annual Review of Neuroscience 30, 535–574.

Holmgren, N.M.A., Olsson, O., 2000. A three-neuron model of information processing during Bayesian foraging. In: Malmgren, H., Borga, M., Niklasson, L. (Eds.), Perspectives in Neural Computing: Artificial Neural Networks in Medicine and Biology. Springer, London, pp. 265–270.

Houston, A.I., McNamara, J.M., Kacelnik, A., 1982. Some learning rules for acquiring information. In: McFarland, D. (Ed.), Functional Ontogeny. Pitman, London, pp. 140–191.

Kacelnik, A., Krebs, J.R., 1985. Learning to exploit patchily distributed food. In: Sibly, R.M., Smith, R.H. (Eds.), Behavioural Ecology. Blackwell, Oxford, pp. 189–205.

Knill, D.C., Pouget, A., 2004. The Bayesian brain: the role of uncertainty in neural coding and computation. Trends in Neurosciences 27, 712–719.

Kording, K., 2007. Decision theory: What ‘‘should’’ the nervous system do? Science 318, 606–610.

Kording, K.P., Wolpert, D.M., 2004. Bayesian integration in sensorimotor learning. Nature 427, 244–247.

Mangel, M., 1990. Dynamic information in uncertain and changing worlds. Journal of Theoretical Biology 146, 317–332.

Manning, A., 1967. The control of sexual receptivity in female Drosophila. Animal Behaviour 15, 239–250.

McNamara, J.M., Green, R.F., Olsson, O., 2006. Bayes’ theorem and its applications in animal behaviour. Oikos 112, 243–251.

McNamara, J.M., Houston, A.I., 1987. Memory and the efficient use of information. Journal of Theoretical Biology 125, 385–395.

Rodriguez-Girones, M.A., Vasquez, R.A., 1997. Density-dependent patch exploitation and acquisition of environmental information. Theoretical Population Biology 52, 32–42.

Stephens, D.W., Brown, J.S., Ydenberg, R.C., 2007. Foraging: Behavior and Ecology. University of Chicago Press, Chicago.

Valone, T.J., 2006. Are animals capable of Bayesian updating? An empirical review. Oikos 112, 252–259.

van Gils, J.A., Schenk, I.W., Bos, O., Piersma, T., 2003. Incompletely informed shorebirds that face a digestive constraint maximize net energy gain when exploiting patches. American Naturalist 161, 777–793.

Wolfram Research, Inc. 2007. Mathematica, Version 6, Champaign, IL.

Yang, T., Shadlen, M.N., 2007. Probabilistic reasoning by neurons. Nature 447, 1075–1080.

Ydenberg, R.C., Brown, J.S., Stephens, D.W., 2007. Foraging: an overview. In: Stephens, D.W., Brown, J.S., Ydenberg, R.C. (Eds.), Foraging: Behavior and Ecology. University of Chicago Press, Chicago, pp. 1–28.